Inorganic Chemistry

Article

pubs.acs.org/IC

Nickel(II)-Induced Excimer Formation of a Naphthalene-Based Fluorescent Probe for Living Cell Imaging

Arnab Banerjee,[†] Animesh Sahana,[†] Subarna Guha,[†] Sisir Lohar,[†] Ipsit Hauli,[‡] Subhra Kanti Mukhopadhyay,[‡] Jesús Sanmartín Matalobos,*[,§] and Debasis Das*[,†]

[†]Department of Chemistry and [‡]Department of Microbiology, The University of Burdwan, Burdwan 713104, West Bengal, India

[§]Departamento de Química Inorgánica, Facultade de Química, Universidade de Santiago de Compostela, Avenida Das Ciencias s/n, 15782 Santiago de Compostela, Spain

Supporting Information

ABSTRACT: Ni^{2+}-induced intramolecular excimer formation of a naphthalene-based novel fluorescent probe, 1-[(naphthalen-3-yl)methylthio]-2-[(naphthalen-6-yl)methylthio]-ethane (**L**), has been investigated for the first time and nicely demonstrated by excitation spectra, a fluorescence lifetime experiment, and ^1H NMR titration. The addition of Ni^{2+} to a solution of **L** (DMSO:water = 1:1, v/v; λ_{em} = 345 nm, λ_{ex} = 280 nm) quenched its monomer emission, with subsequent enhancement of the excimer intensity (at 430 nm) with an isoemissive point at 381 nm. The fluorescence lifetime of free **L** (0.3912 ns) is much lower than that of the nickel(2+) complex (1.1329 ns). **L** could detect Ni^{2+} as low as 1×10^{-6} M with a fairly strong binding constant, 2.0×10^4 M^{-1}. Ni^{2+}-contaminated living cells of plant origin could be imaged using a fluorescence microscope.

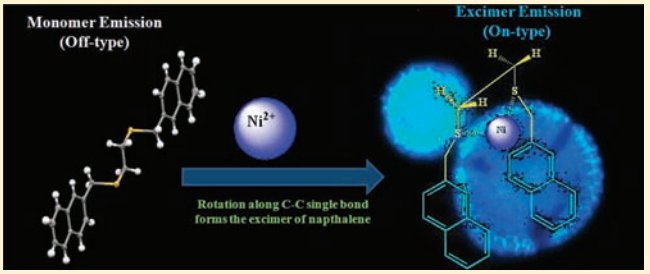

INTRODUCTION

Nickel plays an important role in the biological processes of many microorganisms and plants.[1] Several nickel-containing enzymes and coenzymes, such as urease, Ni−Fe hydrogenases, F430, etc., have a significant role in human life.[2] However, exposure to nickel and its soluble compounds should not exceed 0.05 mg cm^{-3} in nickel equivalents per 40 h work week. Nickel sulfide fumes, dust, and various other nickel compounds are believed to be carcinogenic.[3,4] Although the exact mechanism of nickel imbalance is not very clear, excess nickel accumulation can aberrantly affect respiratory and immune systems. Trace-level Ni^{2+} in living systems can be detected using selective fluorescent probes as cell-imaging reagents.[5,6] Several analytical techniques like atomic absorption or inductively coupled plasma emission/mass spectrometry are available for trace-level determination of nickel, but those methods are not suitable for in vivo study. Recently, fluorescence techniques are being widely used for this purpose. Ni^{2+}-responsive fluorescent probes are rare. Although very few Ni^{2+}-selective peptide,[7,8] protein,[9] polymer,[10,11] and small-molecule-based sensors[12−15] have been reported, but none of them have been utilized for cell imaging. To date, only one BODIPY-based probe has been used for the in vivo study[16] of human cells. Plant systems have an indirect effect on animal systems, and the accumulation of the sensor molecule by the plant cell wall makes the detection of Ni^{2+} more difficult in the plant cell than the animal cell. Moreover, fluorescent sensors that work through a ratiometric mechanism[17] can inherently avoid the effect of surrounding environments like temperature, polarity of media, and probe concentration because the ratios of the two emission intensities (at one, the wavelength intensity increases, while in the other, it decreases) are measured as a function of the externally added cation concentration. To the best of our knowledge, this is the first report of the detection of Ni^{2+} in plant cells with a ratiometric sensor.

Among the few[18−21] reported metal-ion-induced excimer formations, the presence of pyrene fluorophore has been found to be very common, and metal ions involved were Ag^I and Cu^{II}. For the first time, we report the Ni^{2+}-induced intramolecular excimer formation of a naphthalene fluorophore. Naphthalene shows higher red shift (∼150 nm) than pyrene (∼100 nm) upon metal-induced excimer formation and, hence, relatively less interference is observed. The presence of two S atoms (soft donor) in our molecule helps to bind borderline Lewis acid Ni^{2+}.

EXPERIMENTAL SECTION

Materials and Physical Methods. High-purity *N*-(2-hydroxyethyl)piperazine-*N*′-2-ethanesulfonic acid and 2-(bromomethyl)naphthalene were purchased from Sigma Aldrich. Ethane-1,2-dithiol was purchased from Alfa Aesar. Spectroscopic-grade solvents were used. Other chemicals were of analytical reagent grade and were used without further purification except when specified. Milli-Q 18.2 MΩ cm^{-1} water was used throughout all of the experiments. A Jasco (model V-570) UV−vis spectrophotometer

Received: January 18, 2012
Published: May 4, 2012

   dx.doi.org/10.1021/ic300130y | *Inorg. Chem.* 2012, 51, 5699−5704

was used for absorption studies. Fourier transform inafrared (FTIR) spectra were recorded on a Jasco FTIR spectrophotometer (model: FTIR-H_2O). Mass spectra were recorded in a QTOF Micro YA 263 mass spectrometer in electrospray ionization (ESI) positive mode. ^{1}H NMR spectra were recorded using a Bruker Advance 600 (600 MHz) in dimethyl sulfoxide (DMSO)-d_6. The ^{13}C NMR spectrum of 1-[(naphthalen-3-yl)methylthio]-2-[(naphthalen-6-yl)methylthio]ethane (**L**) was recorded using a Bruker Advance 500 MHz instrument in $CDCl_3$. Elemental analyses were performed using a Perkin-Elmer CHN analyzer with a first 2000-Analysis kit. Steady-state fluorescence studies were performed with a Hitachi F-4500 spectrofluorimeter. pH measurements were performed with a Systronics digital pH meter (model 335). All spectra were recorded at room temperature. Single-crystal X-ray structural studies were performed with the following specifications: X-ray data collection, *APEX2* (Bruker AXS, 2005); cell refinement, *APEX2* (Bruker AXS, 2005); data reduction, *APEX2* (Bruker AXS, 2005); program(s) used to solve structure, *SIR97*;[22] program(s) used to refine structure, *SHELXL97*;[23] molecular graphics, *ORTEP-3 for Windows*;[24] software used to prepare material for publication, *WinGX* publication routines.[25] CCDC 805130 contains X-ray crystal structure details of **L**. Time-resolved fluorescence lifetime measurements of **L** and the [**L**-Ni^{2+}] system were carried out using a time-correlated single-photon-counting (TCSPC) spectrometer from IBH (U.K.). The sample was excited at 375 nm by using a picosecond laser diode (IBH, Nanoled), and the signals were collected at the magic angle (54.7°) using a Hamamatsu microchannel plate photomultiplier tube (3809U). The instrument response function of our setup was 110 ps. The same setup was used for anisotropy measurements. Analysis of the data was carried out using IBH DAS, version 6, and decay analysis software.

Imaging System. The imaging system was comprised of an inverted fluorescence microscope (Leica DM 1000 LED), a digital compact camera (Leica DFC 420C), and an image processor (Leica Application Suite v3.3.0). The microscope was equipped with a 50 W mercury lamp.

Preparation of Cells. Pollen grains were obtained from freshly collected mature buds of *Allamanda puberula* (Aapocynaceae), a common ornamental plant with bell-shaped bright-yellow flowers, by crushing stamens on a sterile Petri plate and suspending them in normal saline. After crushing, the stamina debris was removed by filtering through a thin layer of nonabsorbent cotton, and the suspended pollens were collected by centrifugation at 5000 rpm for 5 min. The pollen pellet was then washed twice in normal saline and incubated in a solution of $Ni(ClO_4)_2$ (50 μM) for 1 h at ambient temperature. After incubation, it was again washed in normal saline. After further incubation, the cells were washed again in normal saline and incubated with ligand (10 μM) for 15 min before observation under high-power magnification of a fluorescence microscope. Ligand-treated cells were mounted on a grease-free glass slide and observed under a Leica DM 1000 fluorescence microscope with a UV filter; cells without Ni^{2+} salt treatment but incubated with ligand were used as the control.

To detect intracellular Ni^{2+}, *Candida albicans* cells (IMTECH No. 3018) from an exponentially growing culture in a yeast extract glucose broth medium (pH 6.0; incubation temperature, 37 °C) were centrifuged at 3000 rpm for 10 min, washed twice in normal saline, and then treated with Ni^{2+} salt at 50 μM for 30 min in normal saline. After incubation, the cells were washed again in normal saline, again incubated with **L** (10 μM) for 15 min, and observed under a high-power fluorescence microscope with a UV filter. Cells loaded with **L** but not with Ni^{2+} were used as the control.

Scheme 1

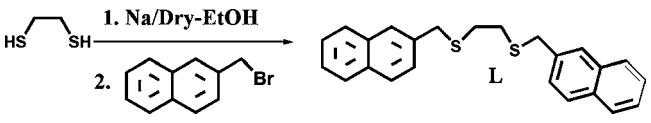

Synthesis of L (Scheme 1). A total of 123 mg (5.31 mmol) of sodium metal was added to 246.7 mg (5.31 mmol) of dry ethanol (EtOH) under an inert N_2 atmosphere with constant stirring until dissolution. To this NaOEt solution, an EtOH solution of ethane-1,2-dithiol (500 mg, 5.31 mmol) was added through a syringe under a N_2 atmosphere with constant stirring for 0.5 h. Then, 1.2 g (5.42 mmol, slight excess over that required to get dimer) of 2-(bromomethyl)-naphthalene was added to the solution, and the solution was stirred for 2 h. Completion of the reaction was confirmed by thin-layer chromatography. The compound was isolated by removing the solvent using a rotary evaporator, followed by solvent extraction with water−ethyl acetate. Then it was purified by column chromatography (hexane:EtOAc = 95:5, v/v). Yield: 75%. Mp: 110 °C (±1 °C). ^{1}H NMR (600 MHz, DMSO-d_6, Figures S1a and S1b in the Supporting Information, SI): δ 2.58 (4H, s), 3.87 (4H, s), 7.43 (2H, m, J = 9.6 Hz), 7.50 (4H, m, J = 3.6 Hz), 7.71 (2H, s), 7.80 (2H, m, J = 9.6 Hz), 7.84 (2H, m, J = 8.4 Hz), 7.88 (2H, m, J = 5.4 Hz). ^{13}C NMR (Figure S2 in the SI, 125 MHz, $CDCl_3$): δ 30.99, 36.74, 125.93, 126.32, 127.08, 127.31, 127.73, 127.78, 128.55. ESI-FIA-TOF HR mass spectral data of **L** ([M + Li]$^+$; Figure S3 in the SI): m/z 381.2969 (found), 381.14 (calcd). Elem anal. Calcd for $C_{24}H_{22}S_2$: C, 76.96; H, 5.92. Found: C, 76.82; H, 5.94. The crystal structure of **L** is presented in Figure 1.

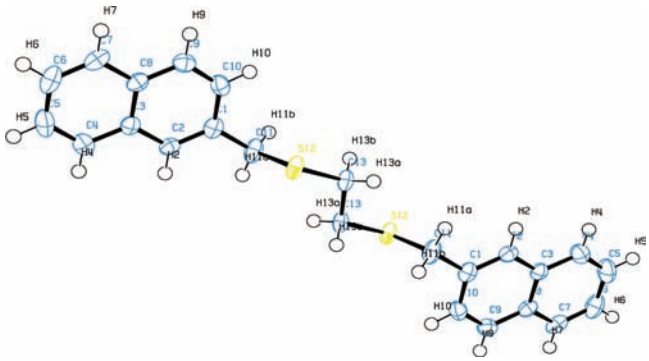

Figure 1. ORTEP view of **L** (the thermal ellipsoid probability is 50%).

RESULTS AND DISCUSSION

Structural Information. Figure 1 presents the crystal structure of **L**, which indicates that two naphthalene units are anti to each other with a 180° torsion angle. Crystal-packing and short-range C−H···π interactions between the naphthalene ring and ethyl protons (H, 13a) are presented in Figures S5 and S6 in the SI, respectively. Single-crystal X-ray structural details are presented in the SI.

Absorption Studies. Changes in the absorbance of **L** as a function of [Ni^{2+}] in a DMSO−water (1:1, v/v, 10^{-5} M) medium are shown in Figure S7 in the SI. Gradual increases of [Ni^{2+}] to the solution of **L** resulted a very low intensity broad band in the visible range (370−460 nm), having a maximum at 420 nm. Another low intensity shoulder appeared at 345 nm.

Emission Studies. **L** shows a monomer emission at 345 nm, characteristic of a naphthalene moiety with a low quantum yield (0.011) in DMSO−water (1:1, v/v, λ_{ex} = 280 nm). The gradual addition of Ni^{2+} to the solution of **L** quenched the monomer emission of the naphthalene moiety, and the intensity of the excimer emission at 430 nm is gradually increased with an isoemissive point at 381 nm (quantum yield 0.013; Figure 2).[26] **L** has a negligible fluorescence intensity at the excitation wavelength of 340 nm, but in the presence of Ni^{2+}, the emission intensity at 430 nm gradually increases (Figure S8 in the SI) with a slightly higher quantum yield

dx.doi.org/10.1021/ic300130y | Inorg. Chem. 2012, 51, 5699−5704

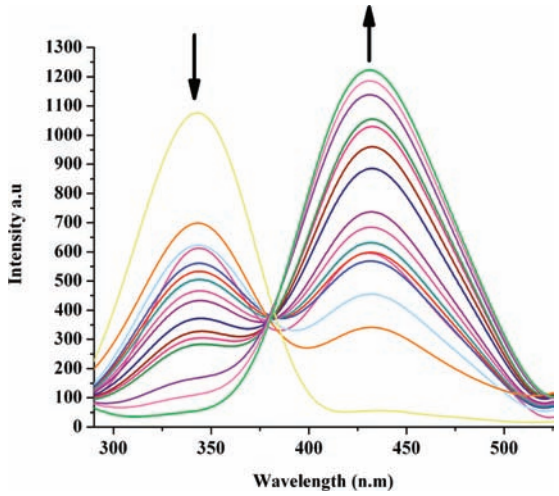

Figure 2. Changes in the emission spectra of **L** (10 μM) upon the addition of Ni^{2+} (10−500 μM, in DMSO−water = 1:1, v/v). λ_{ex} = 280 nm. **L** shows a predominant monomer emission at 345 nm. The concominant addition of Ni^{2+} results a gradual quenching of the emission peak at 345 nm and a gradual increase of the excimer emission at 430 nm.

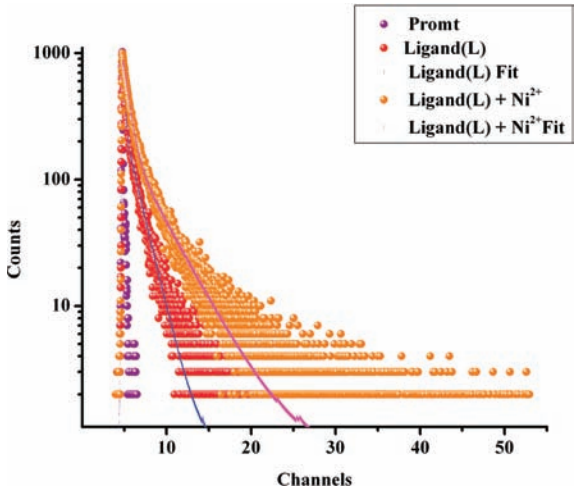

Figure 3. Fluorescence lifetime decay: red dots are due to **L** and golden-yellow dots are due to the [**L**-Ni^{2+}] complex.

Table 1. Fluorescence Lifetime Decay Parameters of L and Its Nickel(II) Complex

	B_1	τ_1(ns)	B_2	τ_2(ns)	$\langle\tau_2\rangle$ (ns)
L	0.115	0.16	0.024	1.5	0.3912
[**L**-Ni^{2+}]	0.08	0.63	0.017	3.5	1.1329

(0.02) at an excitation wavelength of 340 nm rather than excitation at 280 nm (details of the quantum yield calculations are shown in the SI). Evidence of the 430 nm emission assignable to the static excimer of naphthalene is proven by (i) the difference in the excitation spectra (Figure S9 in the SI) of the [**L**-Ni^{2+}] system excited at 345 nm (which corresponds to a naphthalene monomer) and 430 nm (which corresponds to a naphthalene excimer)[27a,b] and (ii) fluorescence lifetime measurement (Figure 3), which shows that the lifetime of free **L** (0.3912 ns) is much lower than the value (1.1329 ns) obtained in the presence of Ni^{2+}. In both cases, only double-exponential decay is observed without any growth, which is

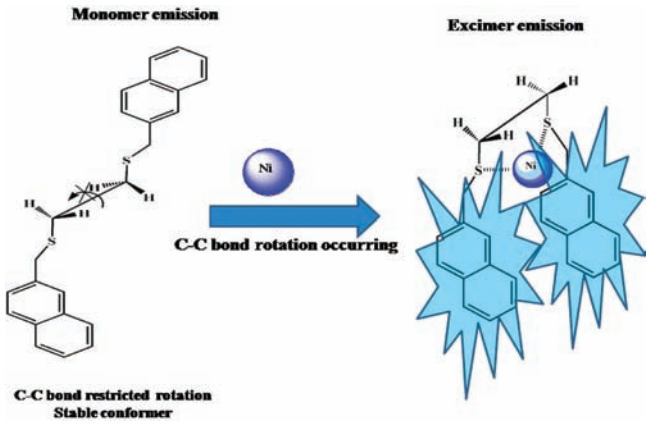

Figure 4. Schematic representation of the plausible mechanism of the Ni^{2+}-induced intramolecular excimer formation of **L**.

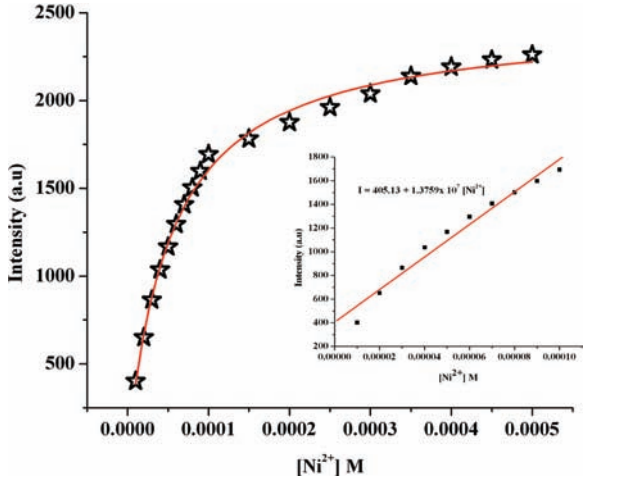

Figure 5. Fluorescence intensity of **L** as a function of the externally added [Ni^{2+}] (10−500 μM). The inset plot may be used for determination of the unknown [Ni^{2+}] (I = 405.13 + 1.3759 × 10^7 [Ni^{2+}]).

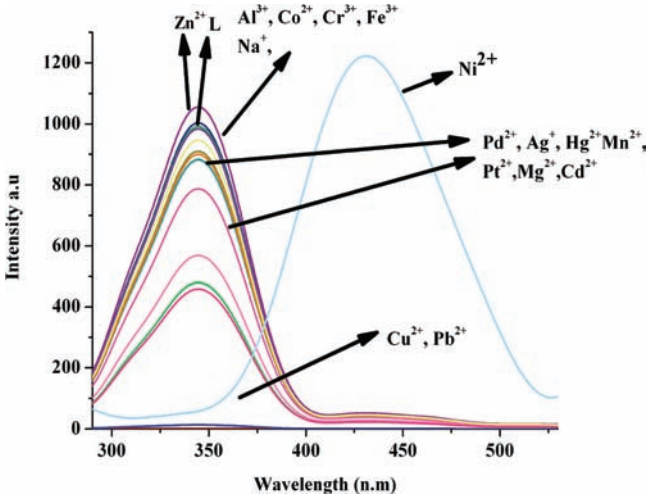

Figure 6. Changes in the fluorescence spectra of **L** (10 μM) in the presence of different metal ions (500 μM). λ_{ex} = 280 nm.

expected[27a] in the case of a dynamic excimer (Table 1). Significant fluorescence enhancement of the [**L**-Ni^{2+}] system is attributed to the attainment of a syn conformation of two

dx.doi.org/10.1021/ic300130y | Inorg. Chem. 2012, 51, 5699−5704

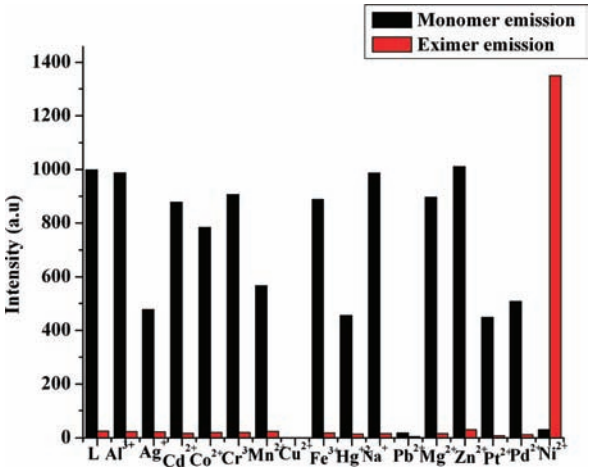

Figure 7. Comparison between the monomer and excimer emissions of **L** and the [**L** + metal ion] systems. λ_{ex} = 280 nm.

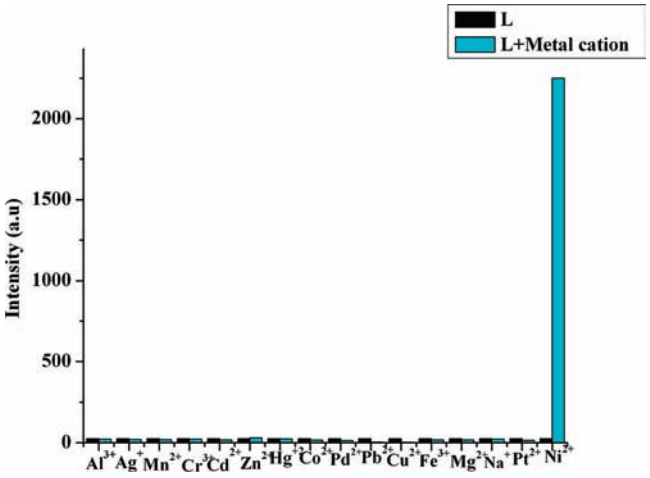

Figure 8. Changes in the fluorescence intensity of **L** (10 μM) in the presence of different metal ions (500 μM). λ_{ex} = 340 nm.

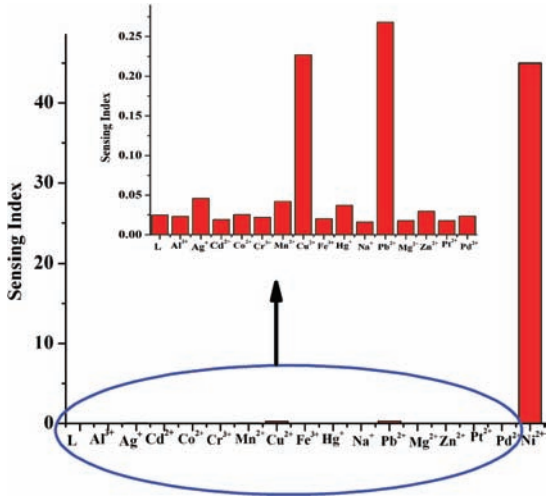

Figure 9. Plot of the sensing indexes (I_{430}/I_{345}) of different metal ions ([**L**] = 10 μM and [metal ions] = 500 μM).

naphthalene rings of **L** in the presence of Ni^{2+}, leading to naphthalene excimer formation (Figure 4). Rotation around the C−C single bond flanked between two S atoms is essential for

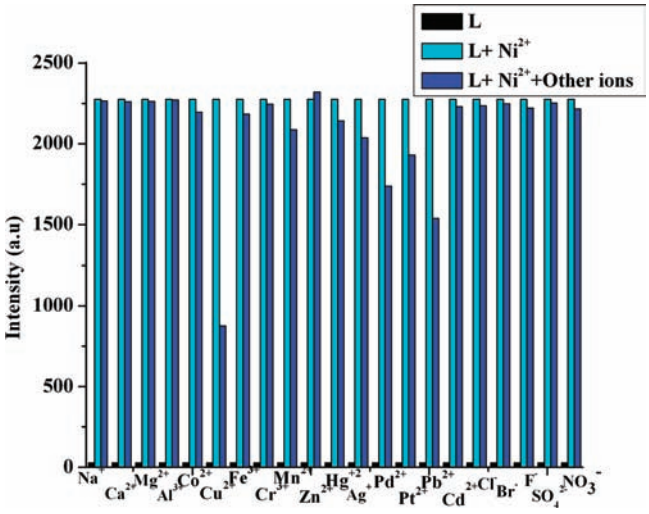

Figure 10. Metal-ion selectivity of **L** (10 μM) in a DMSO−water solution (1:1, v/v) with λ_{ex} = 340 nm. Black bars represent the emission intensity of **L**, sky-blue bars represent the emission intensity of the [**L**-Ni^{2+}] system (1:1, mole ratio), and blue bars show the fluorescence intensity of the [**L**-Ni^{2+}] system (1:1, mole ratio) in the presence of 10 μM of different cations or anions.

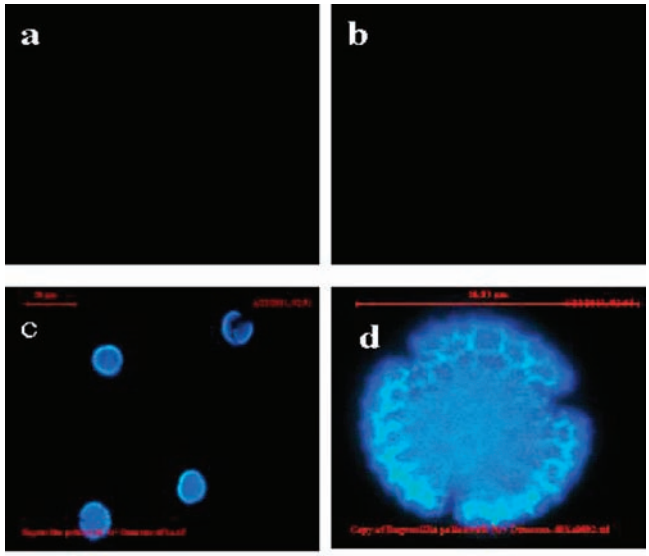

Figure 11. Fluorescence microscopic images of (a) *A. puberula* in the absence of **L**, (b) *A. puberula* treated only with **L**, and (c) *A. puberula* treated with both **L** and Ni^{2+} and (d) an enlarged view of part c.

the binding of **L** to Ni^{2+}. As a result, quenching of the monomeric emission with a large enhancement in the excimer emission of the molecule is observed. ^{1}H NMR titration also supports this fact. The changes in the fluorescence emission intensities (λ_{ex} = 340 nm) of **L** (10 μM) as a function of the added Ni^{2+} concentration are presented in Figure S8 in the SI. The plot of fluorescence intensities versus externally added [Ni^{2+}] (Figure 5) reveals that, over a certain amount of externally added [Ni^{2+}], there is no further change in the emission intensity of the system. Using the inset plot of Figure 5, the unknown concentration of Ni^{2+} can easily be determined as low as 1×10^{-6} M. The high selectivity of **L** for Ni^{2+} over other metal ions is attributed to the affinity of its S atoms for Ni^{2+} and its size and electronic configuration. In the presence of Ni^{2+}, the fluorescence spectrum of **L** (10 μM, λ_{ex} = 280 nm)

dx.doi.org/10.1021/ic300130y | *Inorg. Chem.* 2012, 51, 5699−5704

was distinctly different from those of other metal ions (500 μM) (Figure 6). Figure 7 indicates that the excimer emission intensity of **L** was a maximum for Ni^{2+}, whereas with other metal ions, its monomer emission intensity predominated (λ_{ex} = 280 nm). When **L** was excited in the presence of different metal ions at 340 nm, only Ni^{2+} could produce excimer to a significant extent (Figure 8).

Alkali- and alkaline-earth-metal ions did not interact with **L**. Among other metal ions, Al^{3+}, Fe^{3+}, Cr^{3+}, and Co^{2+} did not show any significant interaction with **L**, maybe because of their hardness. Hg^{2+}, Ag^{+}, Pd^{2+}, Pt^{2+}, Pb^{2+}, Cu^{2+}, Cd^{2+}, Mg^{2+}, and Mn^{2+} show quenching of monomer fluorescence, but no excimer emission of **L** has been observed. The quenching of monomer naphthalene fluorescence may result from the cation–π interaction between the heavy-metal ion and the electron-rich naphthalene unit or by energy- and/or electron-transfer processes. Heavy-metal-atom effects may also be responsible for the observed quenching.[28] The value of the sensing index (I_{430}/I_{345}) for **L** to Ni^{2+} ($[Ni^{2+}]$ = 50[**L**]) is 45.0, whereas it is less than 1 for other metal ions (Figure 9). Job's plot reveals the stoichiometry of the [**L**-Ni^{2+}] system as 1:1 (**L**:Ni^{2+} mole ratio; Figure S10 in the SI) and also supported formation of the mass spectrum of the system (Figure S11 in the SI). The extent of interactions of **L** with Ni^{2+} in DMSO–water (1:1, v/v) has been determined using the modified Benesi–Hildebrand equation[29] (λ_{ex} = 340 nm) as below:

$$1/\Delta F = 1/\Delta F_{max} + (1/K[C]^n)(1/\Delta F_{max})$$

Here $\Delta F = F_x - F_0$ and $\Delta F_{max} = F_\infty - F_0$, where F_0, F_x, and F_∞ are the emission intensities of **L**, in the absence of Ni^{2+}, at an intermediate Ni^{2+} concentration, and at a concentration of complete interaction, respectively. K is the binding constant, [C] is $[Ni^{2+}]$, and n is the number of Ni^{2+} bound per **L** (here n = 1). A plot of $(F_\infty - F_0)/(F_x - F_0)$ versus $[Ni^{2+}]^{-1}$ (Figure S12 in the SI) yielded $K = 2.0 \times 10^4$ M^{-1}.

Developing a highly selective sensor for the analyte over a complex background of potentially competing species is a challenging task. Figure 10 shows the fluorescence response of **L** to Ni^{2+} in the presence of alkali-, alkaline-earth-, and transition-metal ions in DMSO–water (1:1, v/v). Except Cu^{2+}, Pb^{2+}, Pd^{2+}, and Pt^{2+}, other selected coexistent cations did not interfere. Cl^- and SCN^- ions, which did not interfere with the [**L**-Ni^{2+}] system, could mask Pb^{2+}, Pd^{2+}, Pt^{2+}, and Cu^{2+} by forming respective chloro and thiocyanato complexes, respectively. The advantage of the present sensor is that the addition of Ni^{2+} to **L** results in a predominant excimer emission (visible range) over a monomer emission (UV range), giving blue fluorescence, which had not been found earlier.

^{1}H NMR Titration. ^{1}H NMR titration has also supported Ni^{2+}-induced excimer formation of **L** (Figure S13 in the SI). It is well-known that pyrene protons undergo upfield shifts during excimer formation.[30] We have also observed significant upfield shifts for all aromatic protons (nearly 0.1 ppm) of **L** after the addition of Ni^{2+}, but no significant changes have been observed for aliphatic protons (~0.01 ppm). This observation is corroborated from the moderate binding constant value obtained by the fluorescence experiment. Thus, NMR titration not only indicates a weak interaction of the S-donor sites of **L** with Ni^{2+} but also strongly suggests naphthalene excimer formation.

Cell-Imaging Studies. Both Ni^{2+}-contaminated and -free cells have been incubated with **L** and observed under a fluorescence microscope. Figures 11 and S14 in the SI indicate that **L** can permeate living cells tested with no harm because the cells remain alive even after 30 min of exposure to **L** at 10 μM.

CONCLUSIONS

L has been synthesized and characterized by single-crystal X-ray structural studies. Free **L** shows only the monomeric emission, but in the presence of Ni^{2+}, it forms excimer by rotation of the C–C single bond. To the best of our knowledge, it is the first observation of the Ni^{2+}-induced intramolecular excimer formation of two naphthalene rings.

ASSOCIATED CONTENT

Supporting Information

X-ray crystallographic data of **L** in CIF format, synthetic procedures, ^{1}H NMR, ^{13}C NMR, ESI-FIA-TOF HR mass spectra of **L**, other spectral data for **L** and the [**L**- Ni^{2+}] system, and fluorescence microscopic images. This material is available free of charge via the Internet at http://pubs.acs.org.

AUTHOR INFORMATION

Corresponding Author

*E-mail: jesus.sanmartin@usc.es (J.S.M.), ddas100in@yahoo.com (D.D.). Tel: +91-342-2533913. Fax: +91-342-2530452.

Notes

The authors declare no competing financial interest.

ACKNOWLEDGMENTS

The authors sincerely thank West Bengal Council of Science and Technology for financial support. S.G. thanks UGC-DAE-CSR-Kolkata for a fellowship. A.S. and S.L. are thankful to CSIR, New Delhi, India, for providing them fellowship. Authors thank Indian Institute of Chemical Biology (IICB), Kolkata for extending NMR and mass spectrometer facilities. Thanks go to the University Science Instrumentation Center (USIC), Burdwan University, for providing a fluorescence microscope facility. The authors are very thankful to Prof. A. K. Mukherjee, Department of Chemistry, Burdwan University, for helpful discussion and Dr. Nilmoni Sarkar, Department of Chemistry IIT, Kharagpur, for extending the facility of the TCSPC instrument. The authors are also very grateful to the reviewers for their expert opinion, which improved the quality of the manuscript.

REFERENCES

(1) Sigel, A.; Sigel, H.; Sigel, R. K. O. *Nickel and Its Surprising Impact in Nature. Metal Ions in Life Sciences*; Wiley: New York, 2008.

(2) Jaouen, G. *Bioorganometallics: Biomolecules, Labeling, Medicine*; Wiley-VCH: Weinheim, Germany, 2006.

(3) Sunderman, K., Jr.; Salnikow, K. F. W. *Nickel carcinogenesi*; Mutation research, **2003**, *533*, 67.

(4) Dunnick, J. K.; Elwell, M. R.; Radovsky, A. E.; Benson, J. M.; Hahn, F. F.; Nikula, K. J.; Barr, E. B.; Hobbs, C. H. *Comparative carcinogenic effects of nickel subsulfide, nickel oxide, or nickel sulfate hexahydrate chronic exposures in the lung*; Cancer research, **1995**, *55*, 5251.

(5) Domaille, D. W.; Que, E. L.; Chang, C. J. *Nat. Chem. Biol.* **2008**, *4*, 168.

(6) Que, E. L.; Domaille, D. W.; Chang, C. J. *Chem. Rev.* **2008**, *108*, 1517.

(7) Torrado, A.; Walkup, G. K.; Imperiali, B. *J. Am. Chem. Soc.* **1998**, *120*, 609.

(8) Pearce, D. A.; Walkup, G. K.; Imperiali, B. *Bioorg. Med. Chem. Lett.* **1998**, *8*, 1963.

(9) Salins, L. L.; Goldsmith, E. S.; Ensor, C. M.; Daunert, S. *Anal. Bioanal. Chem.* **2002**, *372*, 174.
(10) Wang, B. Y.; Hu, Y. L.; Su, Z. X. *React. Funct. Polym.* **2008**, *68*, 1137.
(11) Wang, B. Y.; Liu, X. Y.; Hu, Y. L.; Su, Z. X. *Polym. Int.* **2009**, *58*, 703.
(12) Fabbrizzi, L.; Licchelli, M.; Pallavicini, P.; Perotti, A.; Taglietti, A.; Sacchi, D. *Chem.—Eur. J.* **1996**, *2*, 75.
(13) Bolletta, F.; Costa, I.; Fabbrizzi, L.; Licchelli, M.; Montalti, M.; Pallavicini, P.; Prodi, L.; Zaccheroni, N. *J. Chem. Soc., Dalton Trans.* **1999**, 1381.
(14) Jiang, L. J.; Luo, Q. H.; Wang, Z. L.; Liu, D. J.; Zhang, Z.; Hu, H. W. *Polyhedron* **2001**, *20*, 2807.
(15) Wang, H.; Wang, D.; Wang, Q.; Li, X.; Schalley, C. A. *Org. Biomol. Chem.* **2010**, *8*, 1017.
(16) Dodani, S. C.; He, Q.; Chang, C. J. *J. Am. Chem. Soc.* **2009**, *131*, 18020.
(17) (a) Ali, M.; Jha, M.; Das, S. K.; Saha, S. K. *J. Phys. Chem. B* **2009**, *113*, 15563. (b) Wang, H. H.; Xue, L.; Qian, Y. Y.; Jiang, H. *Org. Lett.* **2010**, *12*, 292. (c) Lu, C.; Xu, Z.; Cui, J.; Zhang, R.; Qian, X. *J. Org. Chem.* **2007**, *72*, 3554. (d) Wang, J.; Liu, H.; Wang, W.; Kim, I.; Ha, C. *Dalton Trans.* **2009**, 10422. (e) Goswami, S.; Sen, D.; Das, N. K. *Org. Lett.* **2010**, *12*, 856.
(18) Wang, F.; Nandhakumar, R.; Moon, J. H.; Kim, K. M.; Lee, J. Y.; Yoon, J. *Inorg. Chem.* **2011**, *50*, 2240.
(19) Yang, R. H.; Chan, W. H.; Lee, A. W. M.; Xia, P. F.; Zhang, H. K.; Li, K. *J. Am. Chem. Soc.* **2003**, *125*, 2884.
(20) Pandey, M. D.; Mishra, A. K.; Chandrasekhar, V.; Verma, S. *Inorg. Chem.* **2010**, *49*, 2020.
(21) Jung, H. S.; Park, M.; Han, D. Y.; Kim, E.; Lee, C.; Ham, S.; Kim, J. S. *Org. Lett.* **2009**, *11*, 3378.
(22) Altomare, A.; Burla, M. C.; Camalli, M.; Cascarano, G. L.; Giacovazzo, C.; Guagliardi, A.; Moliterni, A. G. G.; Polidori, G.; Spagna, R. *J. Appl. Crystallogr.* **1999**, *32*, 115.
(23) Sheldrick, G. M. *Acta Crystallogr.* **2008**, *A64*, 112.
(24) Farrugia, L. J. *J. Appl. Crystallogr.* **1997**, *30*, 565.
(25) Farrugia, L. J. *J. Appl. Crystallogr.* **1999**, *32*, 837.
(26) (a) McCullough, J. J.; MacInnis, W. K.; Lock, C. J. L.; Faggiani, R. *J. Am. Chem. Soc.* **1982**, *104*, 4644. (b) Morley, K.; Pincock, J. A. *J. Org. Chem.* **2001**, *66*, 2995.
(27) (a) Winnik, F. M. *Chem. Rev.* **1993**, *93*, 58. (b) Martínez, R.; Espinosa, A.; Tárraga, A.; Molina, P. *Org. Lett.* **2005**, *26*, 5869.
(28) Ma, J. C.; Dougherty, D. A. *Chem. Rev.* **1997**, *97*, 1303.
(29) (a) Benesi, H. A.; Hildebrand, J. H. *J. Am. Chem. Soc.* **1949**, *71*, 2703. (b) Banerjee, A.; Sahana, A.; Das, S.; Lohar, S.; Guha, S.; Sarkar, B.; Mukhopadhyay, S. K.; Mukherjee, A. K.; Das, D. *Analyst* **2012**, *137*, 2166.
(30) Nandy, R.; Subramoni, M.; Varghese, B.; Sankararaman, S. *J. Org. Chem.* **2007**, *72*, 938.

dx.doi.org/10.1021/ic300130y | *Inorg. Chem.* 2012, 51, 5699−5704